Intermetallics 30 (2012) 148–153

Contents lists available at SciVerse ScienceDirect

Intermetallics

journal homepage: www.elsevier.com/locate/intermet

Inelastic X-ray scattering in metallic glasses

Pere Bruna [a,f,*], Jorge Serrano [b], Eloi Pineda [c,g], María Jazmín Duarte [a,d], Kun Zhao [e], Wei Hua Wang [e], Daniel Crespo [a,g]

[a] Dpt. de Física Aplicada, Universitat Politècnica de Catalunya, EETAC, C/Esteve Terradas 5, 08860 Castelldefels, Spain
[b] ICREA-Dpt. de Física Aplicada, Universitat Politècnica de Catalunya, EETAC, C/Esteve Terradas 5, 08860 Castelldefels, Spain
[c] Dpt. de Física i Enginyeria Nuclear, Universitat Politècnica de Catalunya, ESAB, C/Esteve Terradas 8, 08860 Castelldefels, Spain
[d] CINVESTAV, Departamento de Materiales, Unidad Querétaro, Querétaro 76230, Mexico
[e] Institute of Physics, Chinese Academy of Sciences, Beijing 100080, China
[f] Centre de Recerca en Nanoenginyeria, Universitat Politècnica de Catalunya, Spain
[g] Centre de Recerca de l'Aeronàutica i de l'Espai, Universitat Politècnica de Catalunya, Spain

ARTICLE INFO

Article history:
Available online 26 April 2012

Keywords:
B. Elastic properties
B. Glasses, metallic
F. Diffraction

ABSTRACT

The behavior of acoustic modes in solids can yield information on the glass dynamics at different length and frequency scales. Inelastic X-ray scattering (IXS) using Synchrotron radiation allows us to obtain detailed information on the sound speed behavior at different length scales as well as approaching the macroscopic limit. This gives an insight to the microscopic mechanisms responsible for the mechanical properties in the THz frequency domain. IXS also provides a method to investigate the fragility of glass-forming liquids via the non-ergodicity factor of the corresponding glasses. Moreover, some questions arise about how phenomena such as the polyamorphism, observed, e.g. in $Ce_{55}Al_{44}$ upon application of pressure, affect the mechanical properties of a metallic glass at a microscopic level. In this article we reveal a change in the high frequency response at the mesoscopic length scale with respect to the ultrasounds limit in metallic glasses. We will also review further applications of IXS on Pd and Ce-based metallic glasses to determine elastic constants, changes in sound speed due to polyamorphism and to investigate their fragility.

1. Introduction

Metallic glasses (MGs) are characterized by their amorphous structure, i.e. their lack of a crystalline lattice, and their metallic character that yields a simpler glassy structure due to the isotropic character of the metallic bonding. These features, offer the opportunity to use bulk metallic glasses in a wide range of novel functional and structural applications, exploiting their magnetic, anti-corrosive or mechanical properties, such as high strength to density ratios and very high restitution coefficients during elastic deformation. Moreover, MGs are ideal systems to study some fundamental aspects of the glassy state, like the mechanisms involved in the Boson Peak and the glass transition.

One way to study these materials is through the study of their collective dynamics. The collective motion of randomly distributed atoms is, at the microscopic level, governed by the interatomic forces between them. Thus, a better knowledge of this interaction leads to a better comprehension of the macroscopic properties of MGs. The collective dynamics of amorphous systems, either liquids or glasses, has been traditionally studied by means of Inelastic Neutron Scattering (INS) [1] but the kinematic limitations of this technique do not allow the study of collective excitations propagating with sound speeds larger than ~1500 m/s [2]. Therefore, MGs, with typical longitudinal sound speeds of around 4000 m/s, have not been studied by inelastic scattering until the advent of third generation Synchrotron radiation sources that provided brilliant X-rays beams with the necessary resolving power to perform Inelastic X-Ray Scattering experiments (IXS). IXS is free of kinematic restrictions, and it yields other advantages with respect to INS; X-rays beams can be focused down to sizes as small as $10 \times 10\ \mu m^2$ allowing the study of very small samples and of materials under extreme pressure and temperature conditions. IXS is the only available technique giving access to the high frequency response of metallic glasses.

The energy spectrum measured by IXS is proportional to the classical atomic dynamic structure factor $S(q,\omega)$, where q and $\hbar\omega$ are the momentum and the energy transfer in the scattering process,

* Corresponding author. Dpt. de Física Aplicada, Universitat Politècnica de Catalunya, EETAC, C/Esteve Terradas 5, 08860 Castelldefels, Spain.
E-mail address: pere.bruna@upc.edu (P. Bruna).

0966-9795/$ – see front matter © 2012 Elsevier Ltd. All rights reserved.
doi:10.1016/j.intermet.2012.03.013

respectively. $S(q,\omega)$ is the space and time Fourier transform of the atomic density–density correlation function and it contains information on the structure and dynamics of atomic systems. In particular, the frequency range of IXS experiments (THz) gives access to the longitudinal sound speed at very small wavelengths. Thus the corresponding sound attenuation coefficients and the elastic moduli of MGs can also be determined. An IXS spectrum for a particular momentum transfer q results in an elastic peak at zero energy due to the frozen density fluctuations and two inelastic peaks at either side of the elastic contribution associated to the creation and annihilation of acoustic excitations. The simplest model to fit this spectrum and, thus, to describe the dynamic structure factor at such high frequencies is the damped harmonic oscillator model (DHO):

$$\frac{S(q,\omega)}{S(q)} = f_q\delta(\omega) + \frac{1-f_q}{\pi}\frac{\Gamma(q)\Omega^2(q)}{\left(\omega^2-\Omega^2(q)\right)^2+\omega^2\Gamma^2(q)} \quad (1)$$

where $S(q)$ is the static structure factor, $\Omega(q)$ is the position of the inelastic peak that corresponds to the maximum of the longitudinal current spectra $C_L(q,\omega) = (\omega/q)^2 S(q,\omega)$, $\Gamma(q)$ is the broadening of the acoustic modes and f_q is the non-ergodicity parameter.

The non-ergodicity parameter is easily obtained from the IXS spectra using the elastic to total integrated intensity ratio of the spectra. In general, f_q depends on the momentum transfer q and the temperature T, and the quantity $1 - f_q$ represents the amount of uncorrelation introduced by the vibrational dynamics. Thus, it is a measure of the amplitude of the vibrations and the degree of disorder of the glass. Scopigno et al. [3] found a link between the non-ergodicity parameter and the kinetic fragility m of the glass, defined in terms of the shear viscosity η_s and the glass transition temperature T_g as:

$$m = \lim_{T\to T_g}\frac{d\log(\eta_s)}{d(T_g/T)} \quad (2)$$

The existence of a relation between m and f_q is interesting not only because it allows measuring the fragility of a liquid from the properties of the glass but because it reveals a link between the slow diffusive properties of the system above T_g and the fast vibrational properties of the glass below T_g. In particular, the temperature dependence of the non-ergodicity factor can be modeled as [3]:

$$f(q\to 0,T)_{T\ll T_g} = \left[1+\alpha\frac{T}{T_g}\right]^{-1} \quad (3)$$

where α is a dimensionless constant parameter that has been empirically correlated to the kinetic fragility through the relationship $m \approx 135\alpha$. Equation (3) is satisfied by very different kinds of glass-forming systems. After the original work by Scopigno et al., only a few glasses deviated from this linear relationship [4,5], mainly fragile systems such as polymeric glass-formers. One of the possible ways to explain the failure of this relation is to assume that it is only valid for systems in which the dynamics of the liquid above T_g is mainly governed by structural relaxation, which is therefore dominating the non-ergodicity of the glassy phase [6]. The presence of secondary relaxations comparable to the structural process would break the correspondence between the ratio of the elastic to the total intensity of the IXS spectra and the non-ergodicity parameter.

The use of IXS to study metallic glasses is very recent and, therefore, it is not clear how MGs fit into this picture. Here, we will examine some of the most prominent results obtained with this technique.

Up to the date, the fragility has been computed from the measure of the non-ergodicity factor in only two systems: $Ni_{33}Zr_{67}$ by Scopigno et al. [7] and $Pd_{77}Si_{16.5}Cu_{6.5}$ by our group [8]. In Section 3.1 we will review these results and we will report new IXS data on another MG, namely $Ce_{70}Al_{10}Ni_{10}Cu_{10}$. Moreover, the temperature dependence of the PdSiCu glass will be presented showing the absence of anharmonic effects on the vibrational properties at room temperature.

Concerning to the mechanical properties, in Section 3.2, we will present the main results obtained in PdSiCu glass comparing samples produced as rods (slow quenching rates) and samples produced as ribbons (ultra-high quenching rates) [9]. The slight difference in density between the two glasses is expected to have pronounced effects on the mechanical behavior, especially in the Young and shear modulus [10].

In Section 3.3 we will exploit the possibility of using small samples with IXS, this allows to study the behavior of MGs under high pressure conditions and to follow the dynamic signatures of pressure-induced polyamorphic transitions. Preliminary results on the pressure dependent behavior of a $Ce_{70}Al_{10}Ni_{10}Cu_{10}$ glass will be presented.

Finally, in Section 3.4, we will discuss recent IXS results on Pd-, Pt-, and Zr-based alloys that have been interpreted as the co-existence of entangled weakly and strongly bound nanoregions with different elastic response [11]. This interpretation assumes a different behavior for metallic glasses than that observed for other kind of glasses. High resolution IXS experiments on the PdSiCu glass will show how this contradiction disappears and how MGs follow the behavior observed for other glasses, i.e. a change in the high frequency response at the mesoscopic length scale with respect to the ultrasound limit.

2. Experimental

Metallic glasses $Pd_{77}Si_{16.5}Cu_{6.5}$ and $Ce_{70}Al_{10}Ni_{10}Cu_{10}$ were prepared by arc melting of pure raw materials in Ar atmosphere and by two different quenching methods: melt spinning and copper mold casting. The melt spinning technique was used for both compositions obtaining ribbons of ~2 mm width and thickness of ~22 and ~40 μm for the PdSiCu and CeAlNiCu glass, respectively. The copper mold casting method was used only for the PdSiCu glass obtaining 1 mm diameter rods. Two discs with thicknesses of ~50 μm were cut for the IXS experiments. The amorphous character of all samples was checked prior to the experiments by synchrotron radiation X-ray diffraction at beamline BM16 at the European Synchrotron Radiation Facility (ESRF). The density of the samples was measured using the Archimedean method with a He pycnometer.

IXS experiments were performed at ESRF beamlines ID28 and ID16. Two kind of experiments were performed, using X-rays of 17.794 keV obtained from the (9 9 9) Si reflection of the monochromator and of 23.724 keV from the (12 12 12) Si reflection. In the first case the photon flux is optimized but at expenses of a low energy resolution of 3 meV whereas in the second case the highest energy resolution of 1.5 meV is obtained but with a reduction in the photon flux. IXS energy scans were performed in the [−40, 40] meV range for momentum transfers between 1.0 and 20 nm^{-1}. The acquisition time ranged between 150 and 300 min per spectrum depending on the photon flux. Several spectra were added in order to reduce statistical noise, and were fitted using equation (1) convolved with the experimental resolution function of the corresponding analyzer and corrected to fulfill the detailed balance condition. The high pressure IXS measurements were performed mounting the CeAlNiCu glass on a diamond anvil cell (DAC) with Ne as a pressure transmitting

medium. Pressure inside the DAC was measured using the ruby fluorescence method.

3. Results and discussion

3.1. Fragility measurements from IXS spectra. Non-ergodicity parameter

Up to the date, IXS has been applied to only few metallic glasses [7–9,11–13]. A typical spectrum obtained at a momentum transfer $q = 2.85$ nm^{-1} for the $Pd_{77}Si_{16.5}Cu_{6.5}$ system is shown in Fig. 1. The main features of IXS spectra are easily identified: the elastic peak at zero energy and the two inelastic peaks at either side of the elastic contribution that correspond to a single acoustic propagating mode. The position of the inelastic peak depends on the value of the momentum transfer. It increases linearly with the momentum transfer at low q, while it begins to bend and finally decreases in energy for q values greater than $q_{max}/2$; where q_{max} is the q value of the maximum of the static structure factor $S(q)$ in the diffraction pattern. Thus, the acoustic excitations follow a dispersion relation, shown in Fig. 2, that allows us to define a pseudo-Brillouin zone limited by $q_{max}/2$. Measuring the IXS spectra for several q values, the non-ergodicity parameter f_q can be computed from the elastic to total intensity ratio: $f_q(Q,T) = I_{el}/I_{tot}$. Therefore, from equation (3), the parameter α that is expected to be related to the fragility can be calculated as:

$$\alpha = \lim_{q\to 0} \alpha(q) = \lim_{q\to 0} \left(\frac{1}{f_q} - 1\right) \frac{T_g}{T} \tag{4}$$

The experimental values of f_q and $\alpha(q)$ are shown in Fig. 3 for the two MGs studied: PdSiCu and CeAlNiCu. The value of α for $q = 0$ was assumed to be that obtained for the lowest momentum transfer, since f_q is known to saturate near $q = 0$ [3]. The value obtained in this way defines an upper limit for α whereas the lower limit would be given by the linear extrapolation of $\alpha(q)$ at $q = 0$. For PdSiCu, with $T_g = 635$ K, the value of α is 0.47(4) while for CeAlNiCu, with $T_g = 359$ K, α is 0.19(4). Assuming that the empirical relation $m = (135 \pm 10)\alpha$ also holds for MGs, the values of the fragility determined by IXS are 63(9) and 26(9) for PdSiCu and CeAlNiCu, respectively. These values are shown in Table 1 and compared to the fragility values obtained from viscosity or calorimetric measurements [14–16]. As it can be seen, the agreement between the m values measured with other techniques is very good. The values obtained from these MGs can be plotted in the m vs α graph together with the points for conventional glasses taken from Ref. [3] (Fig. 4), therefore, these results confirm the validity of the empirical relation between the properties of the liquid above T_g (fragility) and the properties of the corresponding glass below T_g (non-ergodicity parameter) in metallic glasses. Moreover, according to Ref. [6], the existence of this linear relationship in MGs implies that secondary relaxations, although they may be present, are of much less importance than the structural relaxation process.

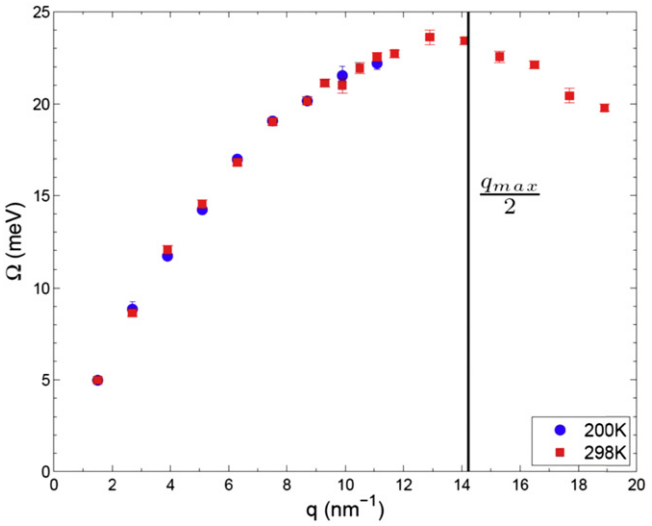

Fig. 2. Dispersion relation for the $Pd_{77}Si_{16.5}Cu_{6.5}$ at two different temperatures. The line signals the position of the q value corresponding to half the q value of the maximum of the static structure factor $S(q)$.

IXS spectra of the PdSiCu glass were obtained both at room temperature (RT = 298 K) and at a lower temperature of 200 K. Low temperature experiments were performed mainly to explore the possible existence of anharmonic effects in the interaction potential between the particles of the system at room temperature. Such effects would be visible as a change in the value of the alpha parameter. Fig. 2 shows that the dispersion relation at 200 K is exactly the same as at RT, whereas the non-ergodicity parameter

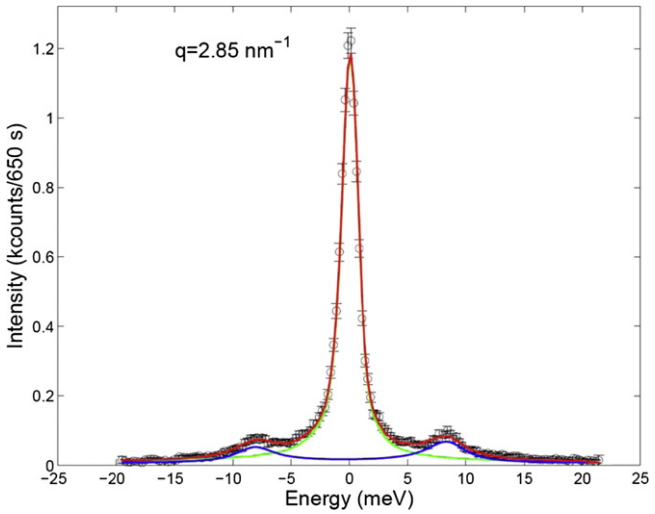

Fig. 1. IXS spectra (circles) for the $Pd_{77}Si_{16.5}Cu_{6.5}$ at $q = 2.85$ nm^{-1}. The best fit to the experimental points (red line) together with the elastic (green line) and inelastic (blue line) contributions are also plotted. (For interpretation of the references to color in this figure legend, the reader is referred to the web version of this article.)

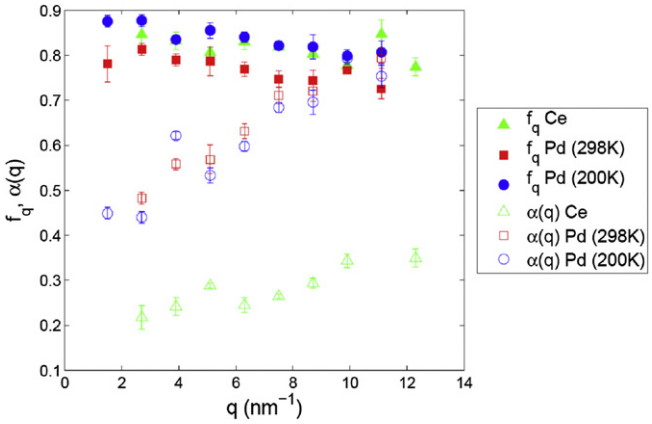

Fig. 3. Non-ergodicity parameter f_q (solid symbols) and the α parameter (open symbols) as a function of the momentum transfer, for the two glasses studied and at two temperatures for the case of the $Pd_{77}Si_{16.5}Cu_{6.5}$. Note how f_q of $Pd_{77}Si_{16.5}Cu_{6.5}$ is greater at lower temperatures.

Table 1
Values of α, fragility determined by IXS and fragility obtained by viscosity and calorimetric measurements.

Alloy	α	$m = 135\alpha$ (IXS)	m (viscosity)	m (calorimetry)
$Pd_{77}Si_{16.5}Cu_{6.5}$	0.47 (4)	63 (9)	75	61
$Ce_{70}Al_{10}Ni_{10}Cu_{10}$	0.19 (4)	26 (9)	–	21
$Ni_{33}Zr_{67}$	0.19 (4)	26 (9)	24	–

shown in Fig. 3 increases, as expected from equation (3). As the elastic contribution is due to the frozen density fluctuations existing in the liquid, it is not affected by the temperature change, while the inelastic scattering contribution is expected to diminish as the temperature decreases and less vibrational modes are excited. Therefore, the total intensity measured in an IXS spectrum at 200 K is smaller than at RT whereas the elastic intensity remains constant, thus increasing the value of the non-ergodicity parameter as can be seen in Fig. 3. However, in the same figure it can be seen how the parameter α, which accounts for the non-ergodicity parameter normalized by temperature, remains, at each q, constant within the experimental uncertainty. Thus, the fragility value obtained at 200 and 298 K is the same, showing that there are no significant effects of anharmonicity up to room temperature.

3.2. Mechanical properties of metallic glasses as a function of the quenching rate

The measure of some mechanical properties is often limited to bulk metallic glasses, where relatively big samples can be produced and, for example, sound velocities can be easily measured by ultrasonic techniques. Therefore, the mechanical properties of MGs produced in ribbon shape with fast quenching methods are not accessible. It is clear that metallic glasses of the same composition but obtained with very different quenching rates (10^1–10^2 K/s versus 10^6 K/s) have different fictive temperatures and lie in a different minimum of the potential energy landscape. Thus, both glasses are expected to have a different degree of spatial homogeneity and the slightly different densities can have a pronounced effect on the Young or the shear moduli [10]. The study of the high frequency response of a PdSiCu system in ribbon form (fast quenched MG) allows to determine their sound velocities and compare them with those obtained for the same system obtained as a rod (BMG); furthermore, the use of the same experimental technique allows a quantitative comparison.

The dispersion relation of the acoustic excitations of the rod and the ribbon are directly obtained from the fitting of the IXS spectra with the DHO model [9]. As no significant differences are observed one can calculate the longitudinal phase velocity as $v_L(q) = \Omega(q)/(\hbar q)$, plotted in Fig. 5. At low q values, the phase velocity should coincide with the macroscopic sound velocity while for higher q's it begins to bend as it is also found in crystals. Looking to Fig. 5 it is clear that the sound speed of the ribbon for medium and low values of q is slightly lower than that of the rod, consistently with the fact that the density of the rod is higher due to the reduction of free volume frozen-in during the quenching process. These velocities can be compared with the macroscopic sound limit that is already known in the case of the rod [17] but it is unknown for the ribbon. Thus, we computed the macroscopic velocities of the ribbon samples from the Debye energy (E_D) [18] and the expressions of the longitudinal and transverse velocities, v_L and v_T, as a function of the bulk modulus B and shear modulus G:

$$\frac{3}{E_D^3} = \frac{1}{6\pi^2\hbar^3 n}\left(\frac{1}{v_L^3} + \frac{2}{v_T^3}\right) \tag{5}$$

$$v_L = \sqrt{\frac{B + \frac{4}{3}G}{\rho}} \quad v_T = \sqrt{\frac{G}{\rho}} \tag{6}$$

where n is the number density and ρ is the density. Although B and G of the ribbon are not known, one can make the assumption than the bulk modulus of the rod and the ribbon are the same because, as it has been found in other MGs [10], the effect of structural relaxation in the elastic constants is much more prominent in the Young and the shear moduli than in the bulk modulus. Thus, using equations (5) and (6) and a value of 174.7(5) GPa for the rod's bulk modulus [17], the shear modulus, the longitudinal and the transversal velocities of the ribbon can be computed and are shown in Table 2. The macroscopic sound speeds of both samples are also plotted in Fig. 5 as a point at $q = 0$. It can be seen how this velocity

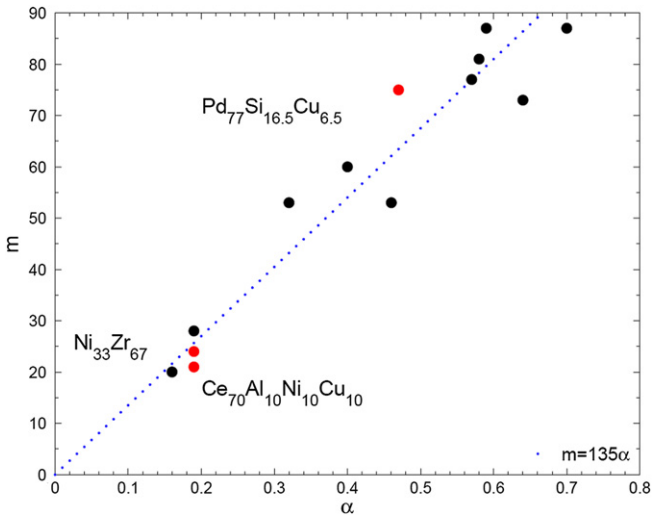

Fig. 4. Comparison of the empiric relation between fragility (m) and the α parameter for conventional glasses (black) and metallic glasses (red). Data of conventional glasses was taken from Ref. [3]. (For interpretation of the references to color in this figure legend, the reader is referred to the web version of this article.)

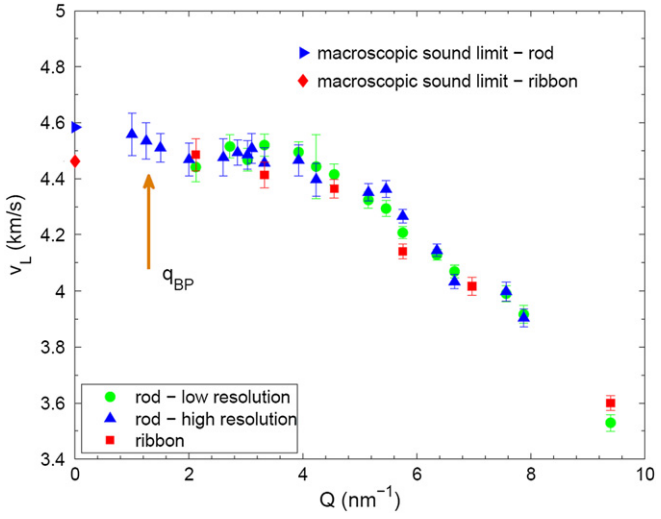

Fig. 5. Longitudinal phase velocity for the $Pd_{77}Si_{16.5}Cu_{6.5}$ metallic glass derived from the IXS experiments with rods and ribbons. The points at $q = 0$ correspond to the macroscopic sound limit obtained from ultrasound methods for the rod and from the elastic constants for the ribbon. The q value corresponding to the boson peak energy (q_{BP}) is also shown.

Table 2
Density (ρ), bulk (B) and shear (G) modulus, longitudinal (v_L) and transverse (v_T) sound velocities and Debye energy (E_D) for $Pd_{77}Si_{16.5}Cu_{6.5}$ rod and ribbon.

Sample	ρ (g cm^{-3})	B (GPa)	G (GPa)	v_L (km s^{-1})	v_T (km s^{-1})	E_D (meV)
Rod	10.49 (5)	174.7 (5)	32.9 (1)	4.58(5)	1.78(5)	21.3 (6)
Ribbon	10.42 (1)	–	24.59 (2)	4.46 (5)	1.54 (5)	18.2 (2)

is, within experimental error, always greater than the phase velocity obtained from the IXS measurements, although they are very close at low q values as expected. It is worth to note that a positive dispersion of the phase velocity as found in Refs. [11,12] is never present in this PdSiCu glass, neither in the rod nor in the ribbon. Thus, the hypothesis made in Ref. [11,12] that a structure of the glass consisting of regions with different elastic properties would lead to positive dispersions seem to be contradicted by the present results: the rods and ribbons of the PdSiCu glass present the same dynamics notwithstanding the fact that they are structurally different [9]. However, without the use of the highest possible energy resolution in an IXS experiment, it is not possible to be conclusive in this point. This will be further discussed in Section 3.4.

3.3. High pressure IXS measurements of metallic glasses

Until recently, the study of polyamorphic transitions was limited to crystalline materials or to glasses with directional and open coordination environments [19]. These kinds of glassy materials involve open local environments that under hydrostatic pressure change to a more densely packed structure. The possibility of polyamorphism in metallic glasses was thus dismissed due to the non-directional nature of the metallic bonds. However, another source of polyamorphism is a change in the electronic structure and bonding, as it has been first observed in a metallic glass containing Ce ($Ce_{55}Al_{45}$) [20]. After this first system, other metallic glasses containing Ce [21–24] have shown polyamorphism that has been experimentally understood through in situ Ce L_3-edge X-ray absorption spectroscopy [22]. The origin of this polyamorphism lies in the special electronic configuration of Ce, in which the strongly correlated 4f electrons can become delocalized under pressure. This causes a large volume shrinkage, responsible in turn of the change of density of the amorphous phase. As the changes in the electronic band structure should be followed by changes in the phonon dispersion relations and sound velocities, IXS can be used to study the changes in the dynamics of a metallic glass under high pressure. In particular, we studied the $Ce_{70}Al_{10}Ni_{10}Cu_{10}$ system in the 0–25 GPa pressure range and the 0–12 nm^{-1} momentum transfer range. A complete dispersion relation similar to the one shown in Fig. 2, was obtained for each pressure value; the longitudinal macroscopic sound velocity, v_L^{macro} is proportional to the slope of this dispersion relation at $q \rightarrow 0$ nm^{-1}:

$$v_L^{macro} = \lim_{q\to 0} \frac{\Omega(q)}{\hbar q} \tag{7}$$

As the dispersion relation bends at q values close to q_{max}, a better value of the slope at $q \rightarrow 0$ is obtained by fitting the experimental points to a sinusoidal function $\Omega(q) = A \cdot \sin(q)$ where $A = \hbar v_L^{macro}$. The longitudinal macroscopic sound velocity computed by this procedure is plotted in Fig. 6 as a function of the applied pressure. At a low applied pressure (0.4 GPa), a slight decrease in the velocity can be observed. This unusual behavior in a metallic glass (high pressures imply higher sound velocities) has been already observed in a Ce-based BMG [25] and attributed to a covalently bonded local structure. At higher pressures, the normal

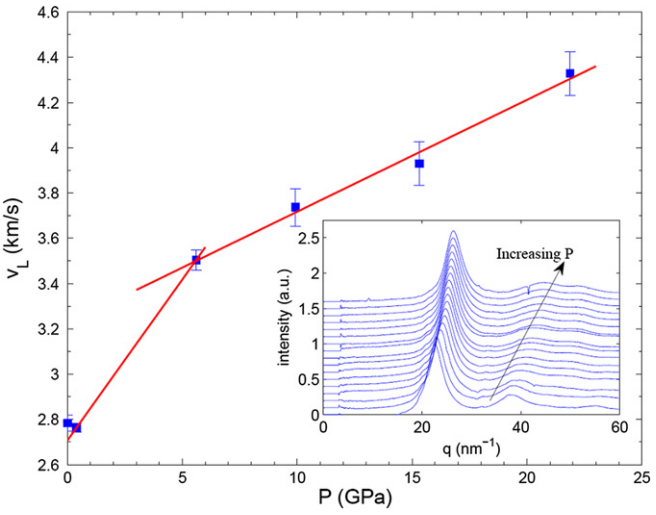

Fig. 6. Evolution of the longitudinal phase velocity as a function of the pressure for the $Ce_{70}Al_{10}Ni_{10}Cu_{10}$ metallic glass. Note the change of slope at around 5 GPa (the lines are guides to the eye). The inset shows the $S(q)$ for several pressures where the position change of the main peak is related to the polyamorphic transition.

positive pressure derivative of the sound velocity is observed. Therefore, according to the changes of the velocity of the acoustic excitations, the transition between two different amorphous phases can be stated. This transformation takes place in the range between 0.2 and 5 GPa and yields a more closed packed atomic configuration with a pressure behavior similar to other metallic glasses. This can be also observed in the position change of the maximum of the $S(q)$ as a function of the pressure, shown in the inset of Fig. 6. The slope of the sound velocity gives an idea of how this transformation occurs. Under application of light pressures the covalently bonded local structure dominates the dynamics and the velocity diminishes. A further increase in pressure is able to break this structure and recover the expected behavior, where the pressure increase is accompanied by an increase of the sound velocity. Next, an outstanding change in the slope of the sound velocity can be observed at around 5 GPa, indicative of a drastic change in the glassy structure. This is the signature of the polyamorphic transition and further analysis will be presented elsewhere [26].

3.4. High frequency response of metallic glasses at the mesoscopic length scale

IXS experiments on metallic glasses allow not only to study their mechanical properties by different ways but also to deepen into theoretical aspects regarding the glass transition or the mechanisms involved in the boson peak [27]. The boson peak (BP) is an excess of vibrational states displayed as a maximum in the reduced vibrational density of states and it is considered the signature of some sort of disorder in the glass. Recent IXS experiments on conventional glasses [28–30] showed a softening of the longitudinal phase velocity, i.e. a rapid decrease with respect the macroscopic sound limit, at the momentum transfer value corresponding to vibrational modes with the energy of the BP (q_{BP}). This negative dispersion contradicts the existing IXS experiments on MGs where the opposite behavior was found [11,12]. Several phenomena could be responsible for this unexpected behavior; between them, the coexistence of strong and weak regions at the nanometer scale was suggested. However, this microscopic description of metallic glasses posed a fundamental dissimilarity between metallic and all other glasses, without a clear physical origin given the relative

simplicity of the metallic potential. Thus, we performed additional IXS measurements on the PdSiCu BMG to shed some light on this problem. High resolution spectra, with energy resolution of 1.5 meV, were collected for momentum transfers as low as 1 nm^{-1}, allowing us to compute the longitudinal phase velocity with high accuracy. Fig. 5 shows the results of these measurements. From this figure it is clear that the metallic glass studied presents a negative dispersion, in accordance with what was found in conventional glasses. Therefore, the use of the IXS technique evidences a common feature in all glasses: a decrease of the phase velocity in the q region where the BP appears that can give some hints on the physical origin of the BP. Moreover, our results on the PdSiCu MG challenge the previous observations on other MGs performed with lower energy resolution [11,12]. Detailed results can be found in Ref. [27].

4. Conclusions

Inelastic X-ray Scattering experiments were performed on two metallic glass compositions with different fragility parameters and under several thermodynamic conditions. This technique offers a microscopic description of the collective dynamics and mechanical properties both for crystalline and amorphous phases. We showed that the fragility parameter of the liquid can be estimated from the non-ergodicity parameter of the corresponding glass and that up to $T \sim 0.5T_g$ there are no anharmonic effects. Moreover, through the determination of the dispersion relation of the acoustic excitations the longitudinal and transverse velocities of metallic glasses produced as ribbons with fast quenching methods was computed and, thus, the elastic constants were determined. High pressure IXS experiments on a Ce-based metallic glass allowed us to unveil a polyamorphic transition through the changes in the vibrational dynamics of the competing amorphous phases. Finally, high energy resolution IXS spectra allowed us to detect a negative dispersion on the phase velocity, thus contradicting the positive dispersion previously found in Refs. [11,12], and giving further evidence of the acoustic origin of the Boson Peak in disordered materials.

Acknowledgments

We acknowledge the beam time granted by the European Synchrotron Radiation Facility, under proposals CRG 16-01-726 and CRG 16-01-702 at BM16, HD-248 and HD-349 at ID28 and inhouse research at ID16. We benefitted from stimulating discussions with J.-B.- Suck, G. Baldi and G. Monaco. We also thank J.J. Suñol for making available his arc-melting setup for sample preparation. This work was supported by CICYT grant MAT2010-14907 and Generalitat de Catalunya grants 2009SGR1225 and 2009SGR1251.

References

[1] Suck J-B, Rudin H, Guntherodt H-J, Beck H. Phys Rev Lett 1983;50:49.
[2] Monaco G. C R Physique 2008;9:608–23.
[3] Scopigno T, Ruocco G, Sette F, Monaco G. Science 2003;302:849–52.
[4] Novikov VN, Ding Y, Sokolov AP. Phys Rev E 2005;71:061501.
[5] Niss K, Dalle-Ferrier C, Giordano VM, Monaco G, Frick B, Alba-Simionesco C. J Chem Phys 2008;129:194513.
[6] Scopigno T, Cangialosi D, Ruocco G. Phys Rev B 2010;81:100202(R).
[7] Scopigno T, Suck J-B, Angelini R, Albergamo F, Ruocco G. Phys Rev Lett 2006; 96:135501.
[8] Serrano J, Pineda E, Bruna P, Labrador A, le Tacon M, Krisch M, et al. J Alloys Comp 2010;495:319–22.
[9] Bruna P, Baldi G, Pineda E, Serrano J, Duarte MJ, Crespo D, et al. J Alloys Comp 2011;509S:S95–8.
[10] He Y, Schwarz RB, Mandrus D, Jacobson L. J Non-Cryst Solids 1996;205–207: 602–6.
[11] Ichitsubo T, Itaka W, Matsubara E, Kato H, Biwa S, Hosokawa S, et al. Phys Rev B 2010;81:172201.
[12] Ichitsubo T, Hosokawa S, Matsuda KK, Matsubara E, Nishiyama N, Tsutsui S, et al. Phys Rev B 2007;76:140201(R).
[13] Nakashima S, Kawakita Y, Otomo T, Suenaga R, Baron AQR, Tsutsui S, et al. J Phys Conf Ser 2007;92:012136.
[14] Perera DN. J Phys Cond Matter 1999;11:3807.
[15] Jiang M, Dai L. Phys Rev B 2007;76:054204.
[16] Guerdane M. Ph.D. Thesis, University of Göttingen; 2000.
[17] Chen HS, Krause JT, Coleman E. J Non-Cryst Solids 1975;18:157–71.
[18] Unpublished results.
[19] McMillan PF, Wilson M, Daisenberger D, Machon D, et al. Nat Mat 2005;4: 680–4.
[20] Sheng HW, Liu HZ, Cheng YQ, Wen J, Lee PL, Luo WK, et al. Nature 2007;6: 192–7.
[21] Zeng QS, Li YC, Feng CM, Liermann P, Somayazulu M, Shen GY, et al. PNAS 2007;104:13565–8.
[22] Zeng QS, Ding Y, Mao WL, Yang W, Sinogeikin SV, Shu J, et al. Phys Rev Lett 2010;104:105702.
[23] Zeng QS, Struhkin VV, Fang YZ, Gao CX, Luo HB, Wang XD, et al. Phys Rev B 2010;82:054111.
[24] Zeng QS, Fang YZ, Lou HB, Gong Y, Wang XD, Yang K, et al. J Phys Condens Matter 2010;22:375404.
[25] Zhang B, Wang RJ, Wang WH. Phys Rev B 2005;72:104205.
[26] Duarte MJ, Bruna P, Pineda E, Crespo D, Garbarino G, Verbeni R, et al. Phys Rev B 2011;84:224116.
[27] Bruna P, Baldi G, Pineda E, Serrano J, Suck J-B, Crespo D, et al. J Chem Phys 2011;135:101101.
[28] Baldi G, Giordano VM, Monaco G, Ruta B. Phys Rev Lett 2010;104:195501.
[29] Ruta B, Baldi G, Giordano VM, Orsingher L, Rols S, Scarponi F, et al. J Chem Phys 2010;133:041101.
[30] Monaco G, Giordano VM. Proc Nat Acad Sci 2009;106:3661.